Research Article | Vol. 25, No. 17 | 21 Aug 2017 | OPTICS EXPRESS 19807
Optics EXPRESS

Origins of Kerr phase and orientational phase in polymer-dispersed liquid crystals

CHIA-MING CHANG,[1] YI-HSIN LIN,[1,4] VICTOR RESHETNYAK,[2] CHUI HO PARK,[3] RAMESH MANDA,[3] AND SEUNG HEE LEE[3,5]

[1]*Department of Photonics, National Chiao Tung University, Hsinchu 30010, Taiwan*
[2]*Theoretical Physics Department, Taras Shevchenko National University of Kyiv, Kyiv 01033, Ukraine*
[3]*Department of BIN Convergence Technology and Department of Polymer Nano-Science and Technology, Chonbuk National University, Jeonju, Jeonbuk 561-756, South Korea*
[4]*yilin@mail.nctu.edu.tw*
[5]*lsh1@chonbuk.ac.kr*

Abstract: Polymer-dispersed liquid crystals (PDLCs) modulate the amplitude and optical phase of light. The optical phase modulation of PDLC can be dissected into two parts: Kerr phase and orientational phase according to the electro-optical (EO) response. We investigated the origins of the Kerr and orientational phases in PDLCs and their connection with the two-step EO response. The Kerr phase is attributed to LC orientation in the center of LC droplets. The orientational phase results from orientation of LC molecules near LC–polymer interfaces. Both phases can be adjusted by varying the droplet size. The two-step EO response in small droplets (<333 nm) is related to the Kerr and orientational phases, and possibly to rotation of point defects. A modified PDLC model considering the Kerr and orientational phases is proposed. Our findings suggest the possibility of versatile photonic devices using pure optical phase modulation.

OCIS codes: (160.3710) Liquid crystals; (190.3270) Kerr effect; (230.0250) Optoelectronics.

References and links

1. J. W. Doane, N. A. Vaz, B. G. Wu, and S. Zumer, "Field controlled light scattering from nematic microdroplets," Appl. Phys. Lett. **48**(4), 269–271 (1986).
2. J. Fergason, "Polymer encapsulated nematic liquid crystals for display and light control applications," Soc. Inf. Disp. Int. Symp. Dig. Tech. Pap. **16**, 68 (1985).
3. P. Chanclou, B. Vinouze, M. Roy, and C. Cornu, "Optical fibered variable attenuator using phase shifting polymer dispersed liquid crystal," Opt. Commun. **248**(1–3), 167–172 (2005).
4. C. Levallois, B. Caillaud, J. L. de Bougrenet de la Tocnaye, L. Dupont, A. Lecorre, H. Folliot, O. Dehaese, and S. Loualiche, "Nano-polymer-dispersed liquid crystal as phase modulator for a tunable vertical-cavity surface-emitting laser at 1.55 μm," Appl. Opt. **45**(33), 8484–8490 (2006).
5. H. W. Ren, Y. H. Fan, Y. H. Lin, and S. T. Wu, "Tunable-focus microlens arrays using nanosized polymer-dispersed liquid crystal droplets," Opt. Commun. **247**(1-3), 101–106 (2005).
6. S. Massenot, R. Chevallier, J.-L. de Bougrenet de la Tocnaye, and O. Parriaux, "Tunable grating-assisted surface plasmon resonance by use of nano-polymer dispersed liquid crystal electro-optical material," Opt. Commun. **275**(2), 318–323 (2007).
7. S. G. Kang and J. H. Kim, "Optically-isotropic nanoencapsulated liquid crystal displays based on Kerr effect," Opt. Express **21**(13), 15719–15727 (2013).
8. S. S. Gandhi and L. C. Chien, "High transmittance optical films based on quantum dot doped nanoscale polymer dispersed liquid crystals," Opt. Mater. **54**, 300–305 (2016).
9. P. S. Drzaic, *Liquid Crystal Dispersions* (World Scientific, 1995), Chap. 4.
10. F. Simoni, *Nonlinear Optical Properties of Liquid Crystals and Polymer Dispersed Liquid Crystals* (World Scientific, 1997), Chap. 5.
11. D. K. Yang and S. T. Wu, *Fundamentals of Liquid Crystal Devices* (John Wiley & Sons, 2006), Chap. 11.
12. S. Zumer and J. W. Doane, "Light scattering from a small nematic droplet," Phys. Rev. A Gen. Phys. **34**(4), 3373–3386 (1986).
13. S. Zumer, "Light scattering from nematic droplets: Anomalous-diffraction approach," Phys. Rev. A Gen. Phys. **37**(10), 4006–4015 (1988).
14. H. Ren, Y. H. Lin, Y. H. Fan, and S. T. Wu, "Polarization-independent phase modulation using a polymer-dispersed liquid crystal," Appl. Phys. Lett. **86**(14), 141110 (2005).

#300925 https://doi.org/10.1364/OE.25.019807
Journal © 2017 Received 27 Jun 2017; revised 2 Aug 2017; accepted 2 Aug 2017; published 7 Aug 2017

Optics EXPRESS

15. G. B. Hadjichristov, Y. G. Marinov, and A. G. Petrov, "Gradient polymer-disposed liquid crystal single layer of large nematic droplets for modulation of laser light," Appl. Opt. **50**(16), 2326–2333 (2011).
16. D. E. Lucchetta, R. Karapinar, A. Manni, and F. Simoni, "Phase-only modulation by nanosized polymer-dispersed liquid crystals," J. Appl. Phys. **91**(9), 6060–6065 (2002).
17. F. Basile, F. Bloisi, L. Vicari, and F. Simoni, "Optical phase shift of polymer-dispersed liquid crystals," Phys. Rev. E Stat. Phys. Plasmas Fluids Relat. Interdiscip. Topics **48**(1), 432–438 (1993).
18. M. J. Sansone, G. Khanarian, T. M. Leslie, M. Stiller, J. Altman, and P. Elizondo, "Large Kerr effects in transparent encapsulated liquid crystals," J. Appl. Phys. **67**(9), 4253–4259 (1990).
19. S. W. Choi, S. I. Yamamoto, Y. Haseba, H. Higuchi, and H. Kikuchi, "Optically isotropic-nanostructured liquid crystal composite with high Kerr constant," Appl. Phys. Lett. **92**(4), 043119 (2008).
20. S. Aya, K. V. Le, F. Araoka, K. Ishikawa, and H. Takezoe, "Nanosize-induced optically isotropic nematic phase," Jpn. J. Appl. Phys. **50**(5R), 051703 (2011).
21. J. Niziol, R. Weglowski, S. J. Klosowicz, A. Majchrowski, P. Rakus, A. Wojciechowski, I. V. Kityk, S. Tkaczyk, and E. Gondek, "Kerr modulators based on polymer-dispersed liquid crystal complexes," J. Mater. Sci. Mater. Electron. **21**(10), 1020–1023 (2010).
22. R. Węgłowski, S. J. Kłosowicz, A. Majchrowski, S. Tkaczyk, A. H. Reshak, J. Pisarek, and I. V. Kityk, "Enhancement of the Kerr response in polymer-dispersed liquid crystal complexes due to incorporation of BiB_3O_6 nanocrystallites," Mater. Lett. **64**(10), 1176–1178 (2010).
23. M. Jiao, J. Yan, and S. T. Wu, "Dispersion relation on the Kerr constant of a polymer-stabilized optically isotropic liquid crystal," Phys. Rev. E Stat. Nonlin. Soft Matter Phys. **83**(4), 041706 (2011).
24. H. Kikuchi, M. Yokota, Y. Hisakado, H. Yang, and T. Kajiyama, "Polymer-stabilized liquid crystal blue phases," Nat. Mater. **1**(1), 64–68 (2002).
25. J. Yan, H. C. Cheng, S. Gauza, Y. Li, M. Jiao, L. Rao, and S. T. Wu, "Extended Kerr effect of polymer-stabilized blue-phase liquid crystals," Appl. Phys. Lett. **96**(7), 071105 (2010).
26. K. M. Chen, S. Gauza, H. Xianyu, and S. T. Wu, "Hysteresis effects in blue-phase liquid crystals," J. Disp. Technol. **6**(8), 318–322 (2010).
27. H. S. Chen, S. Y. Ni, and Y. H. Lin, "An experimental investigation of electrically induced-birefringence of Kerr effect in polymer-stabilized blue phase liquid crystals resulting from orientations of liquid crystals," Appl. Phys. Lett. **101**(9), 093501 (2012).
28. P. S. Drzaic, "Reorientation dynamics of polymer dispersed nematic liquid crystal films," Liq. Cryst. **3**(11), 1543–1559 (1988).
29. S. C. Jain and D. K. Rout, "Electro-optic response of polymer dispersed liquid-crystal films," J. Appl. Phys. **70**(11), 6988–6992 (1991).
30. B. G. Wu, J. H. Erdmann, and J. W. Doane, "Response times and voltages for PDLC light shutters," Liq. Cryst. **5**(5), 1453–1465 (1989).
31. L. Vicari, "Electro-optic phase modulation by polymer dispersed liquid crystals," J. Appl. Phys. **81**(10), 6612–6615 (1997).
32. J. H. Yu, H. S. Chen, P. J. Chen, K. H. Song, S. C. Noh, J. M. Lee, H. Ren, Y. H. Lin, and S. H. Lee, "Electrically tunable microlens arrays based on polarization-independent optical phase of nano liquid crystal droplets dispersed in polymer matrix," Opt. Express **23**(13), 17337–17344 (2015).
33. V. Y. Reshetnyak, T. J. Sluckin, and S. J. Cox, "Effective medium theory of polymer dispersed liquid crystal droplet systems: II. Partially oriented bipolar droplets," J. Phys. D Appl. Phys. **30**(23), 3253–3266 (1997).
34. J. Yan, M. Jiao, L. Rao, and S. T. Wu, "Direct measurement of electric-field-induced birefringence in a polymer-stabilized blue-phase liquid crystal composite," Opt. Express **18**(11), 11450–11455 (2010).
35. R. G. Palmer, D. L. Stein, E. Abrahams, and P. W. Anderson, "Models of hierarchically constrained dynamics for glassy relaxation," Phys. Rev. Lett. **53**(10), 958–961 (1984).
36. J. C. Philips, "Stretched exponential relaxation in molecular and electronic glasses," Rep. Prog. Phys. **59**(9), 1133–1207 (1996).
37. I. C. Khoo and S. T. Wu, *Optics and Nonlinear Optics of Liquid Crystals* (World Scientific, 1993), Chap. 2.
38. D. C. Elton, "Stretched exponential relaxation." (2013).
39. Y. Haseba, H. Kikuchi, T. Nagamura, and T. Kajiyama, "Large electro-optic Kerr effect in nanostructured chiral liquid-crystal composites over a wide temperature range," Adv. Mater. **17**(19), 2311–2315 (2005).

1. Introduction

Polymer-dispersed liquid crystals (PDLCs) are an electro-optical material that modulates the amplitude and phase of incident light; many photonic applications using PDLCs have been developed [1–8]. The well-known mechanism of amplitude modulation by PDLCs is that the incident light is scattered by liquid crystal (LC) droplets randomly dispersed in a polymer matrix when the droplet size is close to the wavelength of incident light. When an external electric field is applied to a PDLC, resulting in changes in the orientations of LC molecules inside the droplets, incident light experiences a match or mismatch between the refractive indices of the LC and polymer, which yields electrically tunable transmittance [9–11]. The

Optics EXPRESS

Rayleigh–Gans approximation is commonly exploited to describe scattering in PDLCs when the LC droplet size is smaller than the light wavelength [9–12]. Anomalous diffraction is used for large droplets [13]. When a high electric field is applied to a PDLC, the scattering effect diminishes, and the modulation of the pure optical phase increases because the incident light sees an average refractive index in the PDLC at high tilt angles of randomly oriented LC molecules [3,14,15]. When the droplet size is much smaller than the wavelength of incident light, for example, nanosize droplets vs. visible light, the nano-PDLC exhibits pure optical phase modulation with polarization independence [15–17]. In 1990, Sansone et al. first discovered the Kerr effect in PDLCs, in which the birefringence of a PDLC is proportional to the square of the electric field, by measuring the phase retardation in PDLCs and proposed that the Kerr effect in PDLCs originates from collective reorientation of the optically anisotropic LC microdroplets, not the electrically polarized LC molecules [18]. Thereafter, many researchers started to study the Kerr effect in PDLCs and attempted to enlarge the Kerr constant of PDLCs [19–23]. For instance, Niziol et al. and Weglowski et al. studied enhancement of the Kerr effect in PDLCs by doping PDLCs with nanocrystallites [21,22]. However, despite reports that the Kerr effect in PDLCs might be attributable to orientation of LC molecules, there has been no clear evidence to date [18]. In addition to LC droplets in PDLCs, blue-phase LCs (BPLCs) consisting of double-twisted cylinders also exhibit the Kerr effect [24–27]. In 2012, we first experimentally demonstrated that the orientation of LC molecules gives rise to the Kerr effect in BPLCs by analyzing the optical phase of BPLCs and the transmittance of dye-doped BPLCs [27]. This finding motivates us to study the relationship between the orientations of LC molecules and the Kerr effect in PDLCs. In this paper, we denote the optical phase shift that is proportional to the square of applied voltage as the Kerr phase. Besides, orientational phase stands for the optical phase shift apart from Kerr phase.

Moreover, the two-step electro-optical (EO) response of PDLCs remains controversial. Some PDLCs exhibit a two-step EO response, whereas others do not [28]. Fergason and Doane et al. discovered PDLCs and developed related applications during 1985 and 1986. Doane et al. first demonstrated experimentally the two-step EO response (i.e., the presence of two slopes in the response time) of PDLCs by measuring the amplitude modulation [1]. Later, Drzaic [28] and Jain and Rout [29] reported similar phenomena. Drzaic proposed a plausible explanation of the two-step EO response: When a small electric field is applied to the PDLC, LC molecules in the center of a droplet start to become reoriented because the anchoring energy has a small effect at the boundary of a droplet. For the same reason, LC molecules in the center of the droplet respond rapidly. When high electric fields are applied to PDLCs, LC molecules near the boundary (i.e., the interface between the polymer and LC) of a droplet are also reoriented by the electric field, and their response is relatively slow because they are constrained by the anchoring energy, or the so-called elastic deformation free energy, provided by the elliptical LC–polymer interface [9–11,16,28,30]. Nevertheless, the explanation does not apply to PDLCs without the two-step EO response. The role of the Kerr effect in the two-step EO response is still unclear. Instead of amplitude modulation of PDLCs, Vicari presented a mathematical model of the optical phase of PDLCs based on the order parameters of LC molecules; the model predicted an optical phase in nano-PDLCs, which agrees well with experiments [31]. However, Vicari did not discuss the two-step EO response or Kerr effect in PDLCs. Recently, we demonstrated electrically tunable focusing microlens arrays of nano-PDLCs with polarization independence [32]. We assign the polarization-independent phase to the orientational phase, in addition to the Kerr phase induced by Kerr effect. Further, the Kerr phase exhibited a smaller phase shift than the orientational phase. The above findings motivate us to investigate the origins of the Kerr and orientational phases in PDLCs and study their role in the two-step EO response.

In this paper, we investigated the origins of the Kerr and orientational phases of PDLCs as well as their connection to the two-step EO response for the first time. We prepared PDLC

Optics EXPRESS

samples with different droplet sizes and analyzed data obtained from measurements of the transmittance, optical phase shifts, and EO response. The experimental results indicate that the Kerr phase is the result of LC orientation in the center of a droplet, which leads to a linear optical phase shift proportional to the square of the electric field. The orientation of LC molecules near the LC-polymer interface makes a major contribution to the orientational phase. The Kerr and orientational phases in PDLC samples could be similar depending on the droplet size. We also found that the two-step EO response occurs in small droplets (<333 nm); in larger droplets, only a single-step EO response occurs. The two-step EO response is indeed related to the Kerr and orientational phases. In addition, the EO responses might be related to the rotations of point defects. We propose a modified PDLC model based on the Kerr and orientational phases in the PDLC samples. The presence of two types of optical phase shifts with different response times in PDLCs would facilitate the design of photonic devices with pure optical phase modulation, such as LC lenses and laser beam steering.

2. Sample preparation and experimental results

The PDLC mixtures consist of a high-dielectric-constant nematic mixture and a photocurable prepolymer. The experimental cell consists of two indium tin oxide (ITO)-coated glass substrates separated by ball-type spacers with diameters of 20 μm. The sheet resistance of ITO-coated glass substrates is around 50~100 Ω/sq. Empty cells are filled with mixtures of the nematic LCs (Merck, MLC-2053, n_e = 1.7472, n_o = 1.5122, Δn = 0.235, $\Delta\varepsilon$ = 42.6, T_{NI} = 86 °C), NOA65 (a UV-curable prepolymer, Norland), and a photoinitiator (Irgacure 907) at different weight percent ratios at 88 °C. Four samples are prepared with LC:NOA65:Irgacure 907 ratios (wt%) of 35:64:1 (sample A), 40:59:1 (sample B), 50:49:1 (sample C), and 55:44:1 (sample D). After the cells are filled with the mixtures, they are cooled to 26 °C and then exposed to UV light (λ = 365 nm) at an intensity of 200 mW/cm^2 for 1 min for photopolymerization. In fact, we can adjust temperature, cooling rate, intensity of UV light, and the exposure time during photopolymerization to control phase separation process for obtaining nano-sized LC droplets in PDLC [11].

To observe the morphologies of the samples by scanning electron microscopy (SEM), the LCs were removed from the samples by soaking the samples in hexane for 48 h, and then the samples were coated with platinum. The thickness of platinum layer is around 1.5 nm (sputtering rate: 1nm/ 60sec). Electron beams with an energy of 5 kV were injected into the samples to obtain SEM images. Figures 1(a)–1(d) show the SEM morphologies of the PDLC samples. The SEM images show that the samples consist of droplets dispersed in the polymer matrix with LCs filling the voids, as presented in Figs. 1(a)–1(d). The average droplet sizes d_{drop} of samples A, B, C, and D are 176, 220, 333, and 483 nm with standard deviations of 23, 63, 83, and 94 nm, respectively. The droplet size increases with increasing LC concentration. The filling factors, defined as the ratios of the area occupied by droplets to the entire area in a SEM image, were calculated from the SEM images using ImageJ, a Java-based image-processing program developed at the National Institutes of Health. The values are 5.6%, 8.6%, 17.3%, and 20.4% for samples A, B, C, and D, respectively. The filling factor rises with increasing LC concentration. On the basis of the filling factors, the volume fractions of LCs in samples A, B, C, and D are 1%, 1.9%, 5.4%, and 6.9%, respectively. However, these values are approximately one-tenth of those calculated from the weight percentage, which are 43%, 49%, 62%, and 68%, respectively. This is probably because some of the LCs are dissolved in the polymer matrix.

Optics EXPRESS

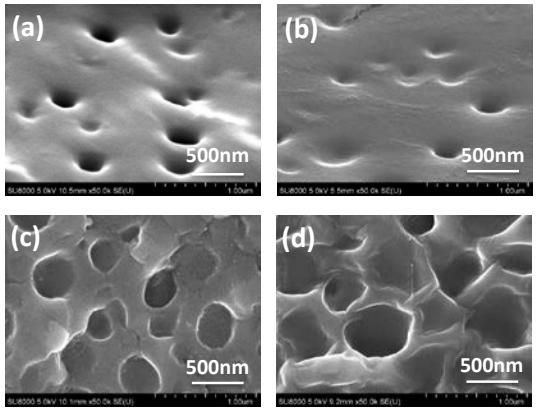

Fig. 1. SEM images of (a) sample A, (b) sample B, (c) sample C, and (d) sample D.

To measure the transmittance of the samples, an unpolarized He-Ne laser (JDSU, Model 1122, λ = 633 nm, TEM_{00} mode, maximum noise = 0.1 rms) irradiated the samples at normal incidence, and a photodetector (New Focus, Model 2031) with a diameter of 8mm was placed 25 cm from the samples to measure the transmitted light while a voltage V was applied to the samples. Figure 2 shows the transmittance of the samples as a function of applied voltage. The transmittances at V = 0 are 87%, 82%, 63%, and 50% for samples A, B, C, and D, respectively. The transmittance increased with increasing applied voltage when the voltage exceeded the threshold voltages (V_{th}), which were ~15 V_{rms} (sample A), ~16 V_{rms} (sample B), ~10 V_{rms} (sample C), and ~8 V_{rms} (sample D). The threshold voltage is reportedly proportional to $1/\sqrt{D}$, where D is the diameter of the LC droplets [33]. The data for our samples fit this relationship with a correlation coefficient of 0.82. Above certain voltages, the transmittance of all the samples saturates at a value exceeding 90%.

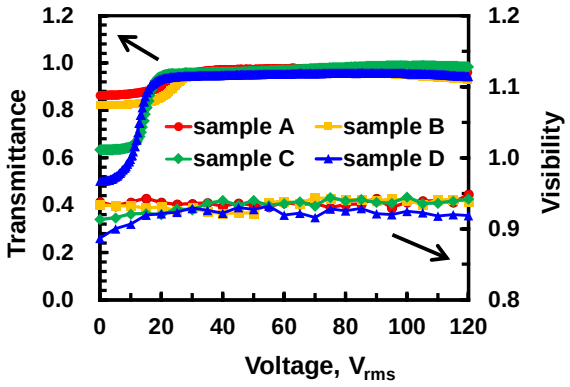

Fig. 2. Transmittance and visibility as functions of an applied voltage.

To identify any scattering in the samples, we measured the visibility of the interference fringes of the samples as well as their optical phase shifts. The optical phase shift and interference fringes were measured and recorded by a Mach–Zehnder interferometer with a two-arm configuration [34]. The samples were placed in one of the arms of the interferometer, and the interference fringes were recorded by a digital camera (Sony, RX100 M3). The interference fringes of the samples at V = 0 and 40 V_{rms} are shown in Fig. 3. For comparison, the interference pattern without a sample is also shown in Fig. 3 (“air”). All of the interference fringes exhibit similar fringe visibility. The visibility of the fringes is defined

Optics EXPRESS

as the ratio of ($I_{max} - I_{min}$) to ($I_{max} + I_{min}$), where I_{max} and I_{min} are the maximum and minimum irradiance of the fringes, respectively. Figure 2 shows the visibility of the four samples as a function of applied voltage. The visibilities of samples A and B (~0.93) are similar to the visibility of fringes without a sample (~0.92). The visibility of sample C is approximately 0.91 at $V = 0$, and that of sample D is slightly lower, ~0.88. Compared to the fringe visibility of ~0.92 with no sample, the fringe visibilities of samples A, B, and C reveal nearly no scattering and indicate pure optical phase modulation under the applied voltage. Figure 1 also provides supporting evidence in terms of the droplet sizes of samples A, B, and C, which are smaller than the laser wavelength. The visibility is less than 1 because of the coherent properties of the laser. For sample D, the scattering is slightly stronger than that of the other samples because the visibility is relatively low, and the size of the droplets is close to the laser wavelength. Nonetheless, sample D shows good visibility in Fig. 3. As a result, we still consider sample D to exhibit good phase modulation. The low transmittance of the samples at $V = 0$ in Fig. 2 is attributed to multiple Fresnel reflections and refractions at the interfaces resulting from the refractive index difference between the LC and the polymer.

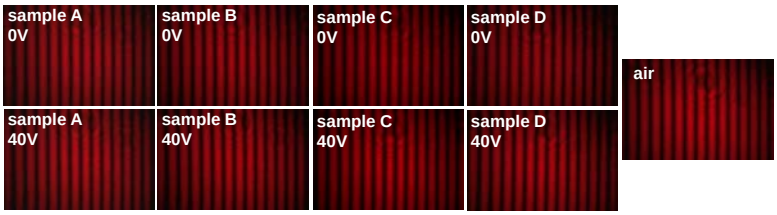

Fig. 3. Interference fringes of samples A, B, C, and D at $V = 0$ and 40 V_{rms} . The right-hand image (air) is the fringe pattern obtained after the samples were removed.

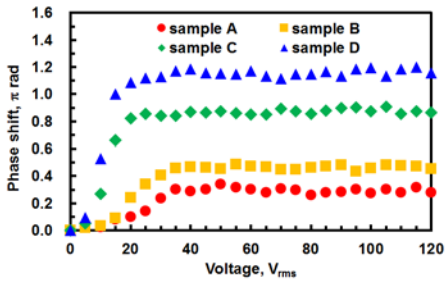

Fig. 4. Phase shift as a function of applied voltage at $\lambda = 633$ nm.

Figure 4 shows the phase shifts as a function of applied voltage for the samples, which were obtained by measuring the fringe shifts and converting them into phase shifts. The total optical phase shifts were 0.277π radians (sample A), 0.455π radians (sample B), 0.865π radians (sample C), and 1.157π radians (sample D). The phase shift increased with increasing droplet size. The results show almost no threshold features in Fig. 4, unlike the results of the transmittance measurement in Fig. 2. In the measurement of the optical phase shift, we used the interferometer to measure the phase accumulation resulting from orientation of LC molecules. In the transmittance measurement (a typical measurement for PDLCs), we used a photodetector to measure the optical intensity resulting from mismatch of the refractive index between the polymer and LC molecules. Although the signals obtained in both the transmittance and phase shift measurements indicate that the effect is related to LC molecular orientation, the interferometer is much more sensitive than the photodetector. The tolerance of optical phase shift is 0.01π radians based on measurements and analysis of the interference fringes shifts. Thus, the phase shift in Fig. 4 indicates small LC orientations as long as the voltage is on. We then converted Fig. 4 to show the optical phase shift vs. E^2, as shown in

Optics EXPRESS

Fig. 5. The optical phase shifts of the samples exhibited linearity at low electric fields when $V < V_{th}$ (here V_{th} is determined from the transmittance measurement), whereas the optical phase shifts deviated from linearity when $V > V_{th}$. The linear phase shift in Fig. 5 indicates the so-called Kerr phase induced by the Kerr effect. The maximum Kerr phases of the samples are the optical phase shifts at $V = V_{th}$, which are 0.08π radians (sample A), 0.092π radians (sample B), 0.271π radians (sample C), and 0.53π radians (sample D). The maximum orientational phase is obtained by subtracting the maximum Kerr phase from the total optical phase shift obtained from Fig. 4. Table 1 lists the maximum Kerr phases and maximum orientational phases, which both increase with increasing droplet size.

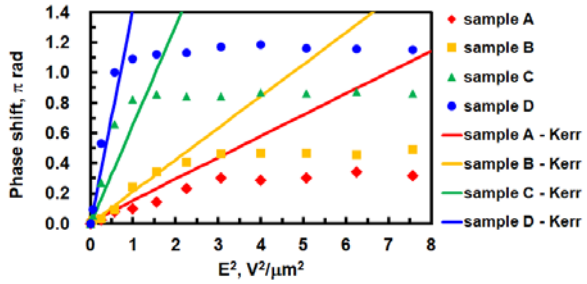

Fig. 5. Phase shift as a function of the square of the electric field (λ = 633 nm). Symbols are experimental results from Fig. 4; solid lines are the Kerr phase based on fitted results of the Kerr effect.

Table 1. Summary of Sample Data.

Sample		A	B	C	D
Threshold voltage, V_{rms}		14.6	16.4	10.4	7.8
Filling factor, %		5.6	8.6	17.3	20.4
Droplet size, nm		176	220	333	483
Theoretical phase shift, radians		0.277π	0.427π	0.856π	1.010π
Total phase shift, radians		0.277π	0.455π	0.865π	1.157π
Maximum Kerr phase shift	**radians**	0.080π	0.092π	0.271π	0.530π
	percentage	28.9%	20.2%	31.3%	45.7%
Maximum Orientation phase shift	**radians**	0.197π	0.363π	0.594π	0.630π
	percentage	71.1%	79.8%	68.7%	54.3%

To examine the response time of the PDLC samples, we measured the response of the samples according to the optical phase shift using a Mach–Zehnder interferometer. A photodetector (New Focus, Model 2031) replaced the digital camera. A voltage of 40 V_{rms} (1 kHz) was applied to the samples and then turned off. The photodetector recorded the corresponding intensity response (or relaxation response), which indicated the optical phase shift of the samples. We used an oscilloscope to record the optical response of the samples. The recorded optical responses were then converted to normalized optical phase shifts. Figure 6 shows the optical phase shift as a function of time, where we turned the voltage off at $t = 0$. To investigate the EO response of the samples, we fitted Fig. 6 using Origin software (OriginLab Corp.). Assuming conventional Debye relaxation [35–37], we fitted the EO response using a combination of two exponential functions: $P(t) = a \cdot \exp^{-(t-t_1)/\tau_1} + b \cdot \exp^{-(t-t_2)/\tau_2}$. $P(t)$ represents the two-step EO response and normalized optical phase shift at a certain time (t); a and b are normalized Kerr and orientational phase obtained from the percentage of phases in Table 1; and t_1 and t_2 are the time delays of the two relaxation responses. Here we set $t_1 = 0$. τ_1 and τ_2 represent the time

Optics EXPRESS

constants of the two relaxation responses. Further, t_2, τ_1, and τ_2 are fitting parameters. The fitted results are plotted in Fig. 6 (red dotted line), and the corresponding fitting parameters are listed in Table 2. τ_1 increases with d_{drop}, but τ_2 first decreases and then increases with increasing d_{drop}. From Table 2, only samples A and B show the two-step EO response, whereas samples C and D do not ($\tau_1 \approx \tau_2$). For samples A and B, the orientational phase corresponds to the first step of the response, whereas the Kerr phase corresponds to the second step. Also, a deviation between fitted function and experimental result was shown in sample D. Instead of Debye relaxation, the response of sample D seems to be stretched exponential relaxation. According to Elton and Phillips [36,38], the stretched exponential relaxation is a result of dynamic heterogeneity which is enhanced with larger LC droplets in sample D.

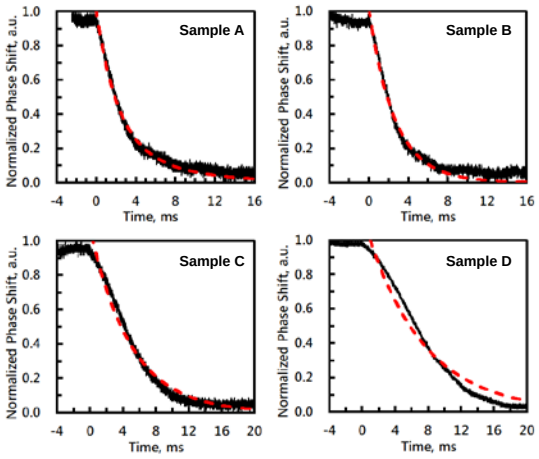

Fig. 6. Optical phase shift of the samples as a function of time, where the voltage (40 V_{rms}) was turned off at t = 0. Black lines show experimental results; red dotted lines are fitting results for $P(t)$.

Table 2. Fitting Parameters of $P(t)$ for Samples

Sample	a	b	t_1	t_2	τ_1	τ_2
A	0.711	0.289	0	0.151	2.028	6.102
B	0.798	0.202	0	0.419	2.397	3.539
C	0.687	0.313	0	1.053	4.934	4.936
D	0.543	0.457	0	1.955	6.955	6.962

3. Discussion

From the droplet diameters and filling factors of the samples shown in Fig. 2, we calculated the total optical phase shift ($\Delta\phi_{theory}$) of the samples at $V >> V_{th}$ according to

$$\Delta\phi_{theory}(V) = \Delta n'(\mathrm{V}) \cdot \frac{2\pi}{\lambda} \cdot d \cdot F, \qquad (1)$$

where F is the filling factor, d is the sample thickness (20 μm), and $\Delta n'$ is the difference between average refractive index [$n_{avg}(V)$] at a particular voltage and the refractive index at V = 0. In Eq. (1), $\Delta n'(\mathrm{V}) \cdot 2\pi \cdot d / \lambda$ is the phase shift when the PDLC is fully occupied by LC droplets (i.e., F = 1). $\Delta n'$ can be written as $\Delta n'(\mathrm{V}) = \left| n_{avg}(V) - \frac{n_e + 2n_o}{3} \right|$. When $V >> V_{th}$,

Optics EXPRESS

$n_{avg}(V) \sim n_0$, and thus $\Delta n'(V) \sim \frac{n_e - n_o}{3}$. Table 1 shows the $\Delta\phi_{theory}$ values of the samples estimated using the experimental parameters F, d, n_e, and n_0. From Table 1 and Fig. 4, the theoretical phase shifts are similar to the experimental results. The error might arise from the variation of d and F. The optical phase shift is largest in sample D because of its larger droplet size and filling factor. From Table 1, we plot the optical phase shift vs. droplet size in Fig. 7. The total optical phase shift increases with increasing droplet size. We attribute this to the increased filling factor for samples with larger droplets. The maximum orientational phase of the samples increases with increasing d_{drop} when d_{drop} < 333 nm and then increases slowly for d_{drop} > 333 nm. However, the maximum Kerr phase does not increase until d_{drop} > 220 nm. As a result, the ratio of the maximum Kerr phase to the total optical phase shift (yellow line with diamonds in Fig. 7) first decreases and then increases as d_{drop} increases, even though the total optical phase shift increases. From Fig. 7, the maximum orientational phase and maximum Kerr phase can have the same order of magnitude if the droplet is large enough. However, too-large droplets would cause light scattering and destroy the pure phase modulation.

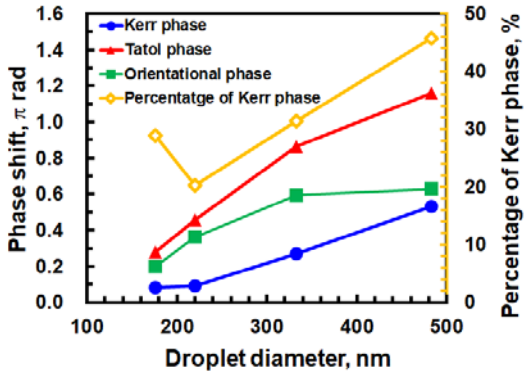

Fig. 7. Phase shift vs. LC droplet diameter.

The Kerr effect is the result of the electrically induced anisotropy when the applied electric field is small, which produces an induced birefringence, $\Delta n_{Kerr}(V) = \lambda \times K \times E(V)^2$, where K is the Kerr constant, and E is the electric field [18]. From Eq. (1), the Kerr phase ($\Delta\phi_{Kerr}$) for $V \le V_{th}$ can be rewritten as

$$\Delta\phi_{Kerr}(V) = \frac{2\pi \times d \times \mathrm{F}}{\lambda} \times \Delta n_{Kerr}(V). \qquad (2)$$

From Eq. (2) and the Kerr phases at $V = V_{th}$ listed in Table 1, we can calculate the Kerr constant: 6.15 × 10^{-8} m/V^2 (sample A), 6.13 × 10^{-8} m/V^2 (sample B), 9.44 × 10^{-8} m/V^2 (sample C), and 1.74 × 10^{-7} m/V^2 (sample D). Then, $\Delta n_{Kerr}(V = V_{th})$ is calculated and is found to be 0.022 (sample A), 0.025 (sample B), 0.015 (sample C), and 0.18 (sample D). The percentage of the maximum birefringence induced by the Kerr effect ($\Delta n_{Kerr}(V_{th}) / (n_e - n_0)$) is 9.32%, 10.57%, 6.36%, and 7.5% for samples A, B, C, and D, respectively. From the calculated Kerr constant, we plotted the Kerr phase $\Delta\phi_{Kerr}$ vs. E^2 in Fig. 5 (solid lines). The Kerr constants of our samples are on the order of ~10^{-7}–10^{-8} m/V^2. The electric-field-induced birefringence of the samples ranges from 0.015 to 0.25, which is similar in order of magnitude to results reported in the literature (~0.025) [18,39]. We further calculated the average refractive index [$n_{ave}(V_{th})$] of the samples at $V = V_{th}$. Here $n_{ave}(V_{th})$ is equal to

Optics EXPRESS

$\Delta n_{\mathrm{ker}\,r}(V_{th}) + n_i$, where n_i is the average refractive index at $V = 0$; $n_i = (n_e + 2n_0)/3 \sim 1.59$, assuming the LC droplets are randomly dispersed in the polymer matrix. As a result, $n_{ave}(V_{th})$ is 1.612, 1.615, 1.605, and 1.608 for samples A, B, C, and D. The results show that the LC molecules in sample D are more highly oriented than those in sample A. This is reasonable because LC molecules are more difficult to reorient in a small droplet.

To investigate the EO response of the PDLCs, we plotted τ_1 and τ_2 as a function of LC droplet diameter (Fig. 8). When $d_{drop} < 333$ nm, the PDLC exhibits a two-step EO response ($\tau_1 \neq \tau_2$). Otherwise, no two-step EO response occurs ($\tau_1 \sim \tau_2$). The total response time, defined as $\tau_1 + \tau_2$, first decreases and then increases with increasing droplet size. Conventionally, the decay time or relaxation time of PDLCs is determined theoretically by balancing three torques: the elastic restoring torque, electric torque, and viscous torque [37]. The corresponding relaxation time of PDLCs follows the relation

$$\tau_{off} = \frac{\gamma_1 \times a^2}{K_{\mathrm{deform}} \times (l^2 - 1)}, \tag{3}$$

where γ_1 is the rotational viscosity coefficient, a is the length of the semimajor axis of a droplet, K_{deform} is the effective deformation constant, and l is the length ratio of the semimajor and semiminor axes. Equation (3) ignores the anchoring effect of droplet interfaces and describes a relaxation similar to nematic relaxation, which results from the dynamics of the Fredericks transition in planar cells. From Table 2, we fitted the relationships between τ_1 and τ_2 and the droplet size and found that $\tau_1 \sim d_{drop}^{2.2}$ and $\tau_2 \sim d_{drop}^{1.46}$ (τ_2 was fitted only for $d_{drop} > 333$ nm). As a result, we can say that the first step of the EO response is similar to the nematic relaxation in Eq. (3) (i.e., $\tau_{off} \sim a^2$). We conclude that the first step of the EO response is related to the orientational phase, and the second step is related to the Kerr phase. Moreover, a PDLC exhibits the two-step EO response when the droplet size is small (<333 nm). The orientational phase responds more quickly than the Kerr phase ($\tau_1 < \tau_2$) for $d_{drop} < 333$ nm. When d_{drop} is large (>333 nm), no two-step EO response occurs in the PDLCs ($\tau_1 \sim \tau_2$). For photonic devices with purely optical phase operation, PDLCs that provide two types of optical phase shifts with different response times can be obtained by adjusting the droplet size.

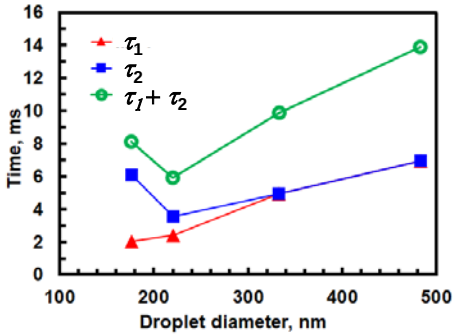

Fig. 8. Time constants of relaxation response in PDLC samples with different droplet size, τ_1 and τ_2, vs. LC droplet diameter.

Next, we suggest a theoretical model to describe the effective refractive index change due to the Kerr phase under an applied voltage. The model assumes that the LC droplets are bipolar with an initially random distribution of the bipolar axis orientation.

Optics EXPRESS

The electrostatic interaction of the LC director n with the electric field E is given by the energy density $F_E = -\frac{1}{8\pi}\varepsilon_a (n\cdot E)^2$, where ε_a is the LC dielectric anisotropy at the frequency of the applied electric field. Under an externally applied electric field, the LC director is reoriented inside each droplet. The LC director reorientation is generally a nonlinear function of the electric field strength. At low field strength, the reorientation is proportional to $\varepsilon_a E^2$ (Kerr phase); at high fields, the director is aligned along the field, and the LC director reorientation saturates. Following a previous work [33], we assume that an individual droplet is spherical and has an initial bipolar axis L_0. There is an elastic energy associated with rotation about this axis, F_{el}. We suppose that the LC interaction with the polymer matrix has a simple phenomenological form:

$$F_{el} = -\pi W R^2 (L\cdot L_0)^2, \tag{4}$$

where the parameter $W > 0$ characterizes the magnitude of the interaction, and R is the droplet radius. We assume that the LC interaction with the polymer matrix is proportional to R^2 because it occurs at the droplet boundary and is therefore likely to scale with the droplet surface area.

At relatively low electric field, the director configuration inside a droplet remains unchanged, but the applied field reorients the bipolar axis of the droplet to a new direction L (Fig. 9) [30]. The initial and final axes of the droplets are described by distribution functions.

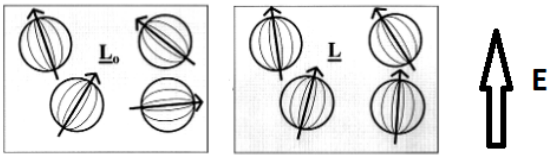

Fig. 9. Schematic illustration of droplets with the electric field off and on. Curved lines in the droplets are director field lines; bold lines indicate the orientation of the bipolar axis.

Within a particular droplet, the distribution of directors is nonuniform. One may describe this nonuniformity in terms of a droplet order parameter *S*:

$$S = \left(\frac{3}{2}(n\cdot L) - \frac{1}{2}\right). \tag{5}$$

If the director field lines within the droplet are surface contours of ellipsoids, S = 0.818 [37]. Then the perpendicular component and anisotropy of the bipolar droplet effective dielectric tensor $\tilde{\varepsilon}$ become [37]

$$\tilde{\varepsilon}_\perp = \varepsilon_\perp + \frac{1}{3}(1-S)\varepsilon_a, \tag{6}$$

$$\tilde{\varepsilon}_a = S\varepsilon_a. \tag{7}$$

To characterize the increasing alignment of the droplets' bipolar axes under the applied electric field, it is convenient to use the bipolar axis order parameter Q [33]:

$$Q = \int_0^{\pi/2}\left(\frac{3}{2}\cos^2\theta - \frac{1}{2}\right)p(\theta,V)\sin\theta d\theta. \tag{8}$$

Optics EXPRESS

For randomly distributed bipolar axes, $Q=0$ (PDLC film in the OFF state); at sufficiently high electric field, Q approaches unity because the bipolar axes all become aligned along the electric field. The order parameter Q depends on the voltage V applied to the PDLC film [33]. One can calculate $Q(V)$ using the results of a previous work [33]. It is desirable to use the nondimensional voltage $\tilde{V}$, which relates $\tilde{V}$ to the applied voltage by the formula [33]

$$\tilde{V}=\left(\frac{\Delta\varepsilon R}{6\pi W}\right)^{1/2}\frac{V}{L}, \tag{9}$$

where

$$\Delta\varepsilon=\frac{\left(\tilde{\varepsilon}_{\perp}+\tilde{\varepsilon}_{a}\right)-\varepsilon_{p}}{\frac{2}{3}+\frac{\tilde{\varepsilon}_{\perp}+\tilde{\varepsilon}_{a}}{3\varepsilon_{p}}}-\frac{\tilde{\varepsilon}_{\perp}-\varepsilon_{p}}{\frac{2}{3}+\frac{\tilde{\varepsilon}_{\perp}}{3\varepsilon_{p}}}. \tag{10}$$

Thus, to obtain the same bipolar axis ordering, one has to apply a voltage that scales as $1/\sqrt{R}$. For the Merck MLC-2053 LCs, $\varepsilon_{\perp}=7.9$ and $\varepsilon_{a}=42.6$, and for NOA65, the dielectric constant is $\varepsilon_{p}\sim 4$. If we take the values $R\sim 10^{-5}cm$, $W\sim 1erg/cm^{2}$, and $L=2\times 10^{-3}cm$ (cell thickness), we obtain $V\approx 0.86\ V$ at $\tilde{V}=1$.

To calculate the phase lag for light passing through the PDLC film, one needs to know the film's effective dielectric tensor at the optical frequency, $\bar{\varepsilon}$. Because the droplets are much smaller than the light wavelength, one can use a Maxwell–Garnett-type theory to describe anisotropic spherical inclusions in an isotropic matrix [33]. However, if the difference between the refractive indices of the LC and polymer matrix is small, the simplest approximation to $\bar{\varepsilon}$ is a linear interpolation. For normally incident light with the polarization along the *x* direction, the effective component $\bar{\varepsilon}_{xx}$ is approximately given by

$$\bar{\varepsilon}_{xx}=\left(1-\eta_{V}\right)n_{p}^{2}+\eta_{V}\varepsilon_{xx,eff}=\left(1-\eta_{V}\right)n_{P}^{2}+\eta_{V}\left\{\varepsilon_{\perp,eff}+\frac{2}{3}\varepsilon_{a,eff}\left[1-Q\left(\tilde{V}\right)\right]\right\}, \tag{11}$$

where n_{p} is the refractive index of the polymer, and η_{V} is the volume fraction of droplets.

Having calculated the bipolar axis order parameter $Q\left(\tilde{V}\right)$, one can find the effective refractive index $n_{eff}\left(\tilde{V}\right)=\sqrt{\bar{\varepsilon}_{xx}}$ and phase shift.

In Fig. 10 we show the phase shift as a function of the nondimensional voltage $\tilde{V}$ for LC droplets with different volume fractions. The refractive index of the polymer matrix is taken to be $n_{p}=1.524$.

Optics EXPRESS

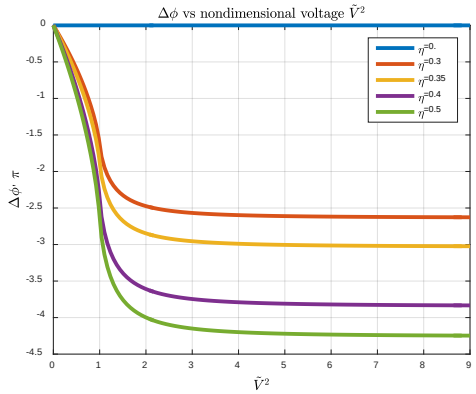

Fig. 10. Phase shift vs. applied electric field for different LC volume fractions.

Up to $\tilde{V} = 0.3$, the phase shift dependence is quadratic, which corresponds to the Kerr phase. At this value of the nondimensional voltage, the phase shift is about 0.2π radians, which seems to be in good agreement with the experiment.

From the experimental results and analysis above, we schematically illustrate the Kerr phase, orientational phase, and EO response of the PDLCs in Figs. 11(a) to 11(f). For PDLCs with small LC droplets (<333 nm), the symmetric axes of LC droplets with bipolar configurations are randomly distributed in the polymer matrix [Fig. 11(a)]. When $V < V_{th}$, the LC molecules at the centers of the LC droplets are reoriented by the electric field, resulting in an optical phase shift that is linearly proportional to the square of the electric field, called the Kerr phase [Fig. 11(b)]. When $V > V_{th}$, the linearity of this optical phase shift is destroyed because more LC molecules in the droplet are aligned parallel to the electric field. The nonlinear optical phase shift at $V > V_{th}$ is the orientational phase [Fig. 11(c)]. The two-step EO response of small droplets reflects the movement of point defects in bipolar droplets [Figs. 11(a) to 11(c)]. Because we adopt the PDLC model of Drzaic [9, 28], the bipolar defects of the droplets are stable when $V < V_{th}$ but rotate when $V > V_{th}$ to minimize the elastic energy [Figs. 11(b) and 11(c)]. For PDLCs with large LC droplets (>333 nm), there is a similar random distribution of LC droplets [Fig. 11(d)]. Because the LC droplets are large, it is relatively easy for LC molecules, including their bipolar point defects, to be reoriented by an applied electric field [Fig. 11(e)]. The linear optical phase shift (Kerr phase) can be measured when $V < V_{th}$ and reaches a maximum when $V = V_{th}$ [Fig. 11(e)]. When $V > V_{th}$, most of the LC molecules in the LC droplets are realigned parallel to the electric field because of the small anchoring energy provided by the spherical (or nonspherical) LC–polymer interfaces [Fig. 11(f)]. The nonlinear optical phase shift for $V > V_{th}$ is the orientational phase [Fig. 11(f)]. For large LC droplets, only a single-step EO response occurs, which is the result of point defect rotation as the voltage turns off. For small LC droplets, the orientational phase responds more rapidly than the Kerr phase. This indicates that relaxation of bipolar point defects occurs more quickly. Instead of explaining the Kerr effect in PDLCs as originating from collective reorientation of the optically anisotropic LC microdroplets, as proposed by Sansone et. al. [18], we provide a more insightful and elaborate model related to the Kerr phase. Compared to conventional light intensity measurement, optical phase measurement using a sensitive interferometer provides more information related to the LC orientation.

Optics EXPRESS

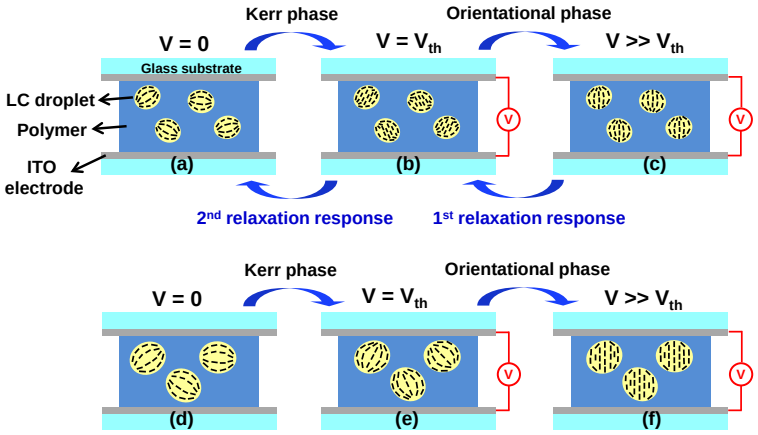

Fig. 11. Kerr and orientational phases in PDLC. (a), (b), (c) PDLC with small LC droplets. (d), (e), (f) PDLC with large LC droplets.

From the droplet volume analysis studies, it is clear that the majority of the liquid crystal remains dissolved in the polymer in samples. The SEM images of the hexane-extracted droplets show clear interface between polymer and the void (Fig. 1). The hexane extraction could cause the polymer to shrink and contract. Instead of distinct boundaries, the polymer/LC interface might be a fuzzy layer of polymer highly swollen with liquid crystals. Near the nematic droplet bulk, the interface could be treated as a nematic with dissolved isotropic contaminant (polymer). Such a swollen LC/polymer layer could still have LC in the nematic phase. Due to the dissolved polymer chains, the order parameter in a swollen LC/polymer layer could be effectively reduced, which would result in a reduction in elastic constants and voltage required for reorientation. As a result, Kerr phase exists as $V< V_{th}$. How fuzzy layer affects the dynamics of PDLC need to be further investigated.

4. Conclusion

We experimentally investigated the origins of the Kerr and orientational phases in PDLCs as well as the correlation between the two optical phases and the two-step EO response for the first time. The Kerr phase, which is linearly proportional to the square of the electric field, is a result of LC orientation in the center of a droplet. The orientational phase arises from orientation of LC molecules near LC–polymer interfaces. The Kerr and orientational phases in PDLC samples can be adjusted by varying the droplet size. We also found that the two-step EO response occurring in small droplets (<333 nm) is indeed related to the Kerr and orientational phases. Rotation of point defects plays a role in the EO response. A modified PDLC model related to the Kerr and orientational phases was also proposed. The proposed theoretical model, which is phenomenological, captures the main features of the Kerr phase and may be used to optimize the PDLC film properties. We believe that, in addition to the conventional features of PDLCs, such as the polarization-independent optical phase shift and response-time-independent cell gap, the Kerr and orientational phases with different response times (approximately milliseconds) in PDLCs pave the way to designing versatile photonic devices with pure optical phase modulation.

Funding

Department of Natural Sciences and Sustainable Development in the Ministry of Science and Technology of Taiwan (MOST) (104-2112-M-009 –010 -MY3); National Research Foundation of Korea (NRF) Basic Science Research Program (2016R1D1A1B01007189)

Optics EXPRESS

Acknowledgments

The authors express appreciation to Mr. Po-Ju Chen and Ms Jing-Yi Wang for technical assistance.